Dissociative recombination of He_2^+ molecular ions

L. Carata* and A. E. Orel
Department of Applied Science, University of California–Davis, Livermore, California 94550

A. Suzor-Weiner
Laboratoire de Photophysique Moléculaire, Université de Paris–Sud, 91405 Orsay, France and Laboratoire de Chimie Physique, 11 rue Pierre et Marie Curie, 75234 Paris, France

(Received 20 October 1998)

We present calculated cross sections and rates for dissociative recombination of the He_2^+ molecular ion in the energy range 0.1 meV–2.0 eV. We used the multichannel quantum defect theory applied to the molecular case, with ionization and dissociation channels simultaneously included. A comparative study has been performed for different isotopic compositions of the He_2^+ ion, different initial rovibrational states of the ion, and three dissociation paths: the lowest dissociative states $^3\Sigma_g^+$, $^1\Sigma_g^+$, and $^3\Pi_u$ of the He_2 molecule for which autoionization widths are obtained by the complex Kohn variational method. [S1050-2947(99)06404-5]

PACS number(s): 34.80.Lx

I. INTRODUCTION

The He_2^+ molecular ion occupies a special place in the study of dissociative recombination (DR). In order to explain the fast recombination rates observed in a helium discharge, Bates [1] suggested that this process, previously proposed for the ionosphere, was important in laboratory plasmas as well. Paradoxically, He_2^+ was later recognized [2] as one of the few molecular ions with a small recombination rate (i.e., much smaller than 10^{-7} $cm^3\,s^{-1}$ at 300 K). Due to the interest in helium discharges and helium afterglows, it has been approached many times from both theoretical and experimental points of view [3–8]. However, no definite absolute cross sections for this process have been presented to date. Experimentally, there have been several measurements of the DR rate in He plasma afterglows [7,8]. Due to the complexity of the phenomena in such media, only controversial results could be obtained. In addition to the difficulties of forming He_2 molecules, it has been shown [7] that in the plasma afterglow most of He_2^+ ions relax rapidly to their ground vibrational level due to various collisional processes. This level seems to have a very low probability of recombination due to the lack of favorable routes for DR near the bottom of the He_2^+ ground-state potential well [3,4]. Experiments on ion storage rings are a promising alternative to the plasma afterglow measurements, and are now being actively pursued [9].

The main scope of the present work is to help in the understanding and measurement of the DR process for He_2^+ ions by studying the influence of various parameters on the DR cross section. First, there are three isotopomers built from the two isotopes ^{3}He and ^{4}He: $^3He_2^+$, $^4He_2^+$, and the mixed variety $^3He^4He^+$. Differences in isotopic composition may prove to be important in the ion storage ring experiments. The heteronuclear ion has a small permanent molecular dipole which permits a more rapid relaxation of vibrationally excited molecular ions. In the case of HD^+ ion this feature was advantageous (as compared to H_2^+) for obtaining an ion beam with a ground vibrational level that is predominantly populated [10–15]. For He_2^+ this advantage can be canceled by the very small DR cross section of ions initially in the ground state, which can make it difficult to measure. On the other hand, an unknown vibrational distribution of the ions in the beam makes a comparison with the theoretical results more difficult. In addition, sources of He_2^+ used for injection of ions into the storage ring produce rotationally *hot* initial distributions, and it is important to check how much the cross section may change with rotational excitation of the target ion.

We thus perform test calculations for various initial rovibrational levels of the ion ground state, and various isotopic combinations of He atoms. We also evaluat the contribution of several closely lying dissociation channels assumed to be the most important at low energy, the lowest $^3\Sigma_g^+$, $^1\Sigma_g^+$, and $^3\Pi_u$ dissociative states of the neutral molecule. Finally, we give the value and the temperature dependence obtained for the DR rate coefficient around room temperature.

II. THEORETICAL APPROACH

The process we study may be summarized by the following reaction scheme:

$$He_2^+(J,v)+e^-\rightarrow\{He_2^*,He_2^{**}\}\rightarrow He+He^*, \qquad (1)$$

where J and v denote, respectively, the initial rotational and vibrational level of the ground-state molecular ion. Since the dissociative recombination process was analyzed in recent review papers [15,16], we only present a brief summary of its main features. One distinguishes two mechanisms: the direct process, when the electron is captured directly into a dissociative state, usually doubly excited (hence the notation He_2^{**}), and the indirect process, when the electron is first captured into a bound Rydberg state He_2^* which is predisso-

*Present address: Laboratoire de Photophysique Moléculaire, Université de Paris–Sud, 91405 Orsay, France. Permanent address: National Institute for Lasers, Plasma and Radiation Physics, Magurele 76900, Romania.

ciated by electronic interaction with the dissociative state He_2^{**}. The indirect process gives rise to sharp resonances in the DR cross section with different shapes depending on the interference with the direct mechanism. A competing process has to be taken into account, namely the autoionization of the intermediate Rydberg He_2^* or doubly excited He_2^{**} neutral molecule, which can fragment back into an electron and a molecular ion in the (J',v') [in general different from (J,v)] rovibrational level

$$He_2^+(J,v)+e^-\rightarrow\{He_2^*,He_2^{**}\}\rightarrow He_2^+(J',v')+e^-. \tag{2}$$

A simultaneous description of these different processes is conveniently handled within the multichannel quantum defect theory (MQDT), extended to the molecular case with dissociative channels in addition to the usual ionization channels [17]. Electronic interactions between singly and doubly excited states (in a quasidiabatic representation of molecular states) are described by a short-range reaction matrix K, evaluated from the electronic couplings within a second-order perturbative approach [18]. Vibrational interactions responsible for the electron capture into monoexcited Rydberg states are treated within a frame-transformation approach between short- and long-range types of coupling for the external electron, and are related to the R dependence of the quantum defect. Rotational interactions could be included in a similar way [19,20], but they usually have a small effect on the size of the cross section [21] and would only be useful for understanding details in high-resolution cross section measurements, when available. In addition, in the specific case of He_2 the Σ-Π angular coupling was shown by Cohen [3] to be much smaller that the radial coupling between pairs of comparable states. In the present calculations we take account of possible initial rotational excitation of the molecular ion, and assume the ion rotational quantum number J to be conserved during the whole process, neglecting angular coupling with the incoming electron. Thus the J and J' values in Eq. (2) are the same, and the corresponding centrifugal potential-energy is added to all the potential energy curves involved in reactions (1) and (2).

Open and closed channels are only distinguished in the last step of the calculations, when the asymptotic conditions are specified. While dissociative states correspond to open channels (open for fragmentation in two atoms), an ionization channel may be open or closed depending if the total energy (ion plus electron) lies above or below its ionization threshold, defined by a given (J,v) level of the ion ground state [cf. Eq. (2)]. Closed channels are responsible for resonances in the cross section, when the total energy coincides with a Rydberg level of a series converging to a ''closed'' ionization threshold.

III. MOLECULAR DATA

The MQDT treatment of DR requires data for the molecular ion curves, the relevant dissociative curves of the neutral molecule, the R-dependent quantum defect, and electronic coupling functions. The ion curves were taken from the *ab initio* calculations of Sunil *et al.* [5]. Entire families of Rydberg states either bound (X core state) or unbound (A core states) were computed by Cohen [3] in a diabatic approach, allowing states of same symmetry and different types (bound or unbound) to cross. The approach used by Cohen to study the inverse process of DR, associative ionization of two He atoms [22], is particularly suitable for our MQDT treatment, as long as the electronic coupling between the crossing states is known, allowing us to calculate the short-range reaction matrix mentioned in Sec. II.

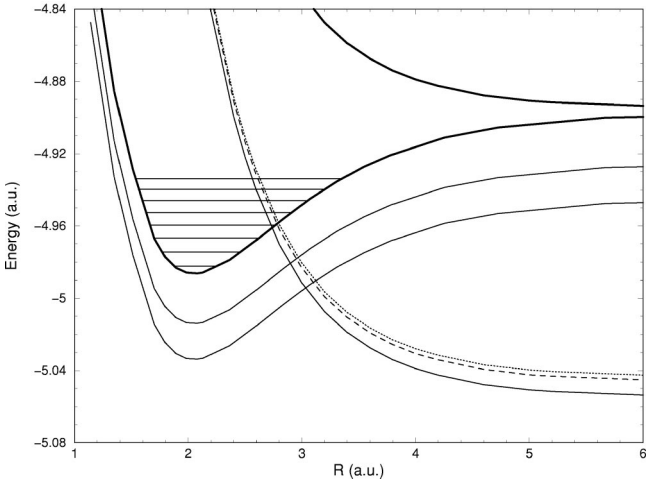

FIG. 1. Potential-energy curves involved in the low-energy DR process of He_2^+. The thick lines correspond to ion states calculated by Sunil *et al.* [5] (the attractive curve is the $X\ ^2\Sigma_u^+$ ion ground state and the repulsive curve is the first excited state $A\ ^2\Sigma_g^+$), and the thin lines represent Rydberg molecular states of the neutral He_2 molecule deduced from the ion core states by appropriate translations. The continuous thin lines have $^3\Sigma_g^+$ symmetry (two $np\sigma_u$ attractive Rydberg states with $n=3$ and 4, and the lowest dissociative state). The dashed line is a dissociative state with $^1\Sigma_g^+$ symmetry, and the dotted line is a dissociative state with $^3\Pi_u$ symmetry. The three dissociative curves are Rydberg states of He_2 with the repulsive state $A\ ^2\Sigma_g^+$ as ionic core.

A. Molecular potential curves

Figure 1 presents the potential curves that have relevance for the dissociative recombination process (1) with slow electrons. Both the ground state $(1\sigma_g^2 1\sigma_u)X\ ^2\Sigma_u^+$ and the repulsive first excited state $(1\sigma_g 1\sigma_u^2)A\ ^2\Sigma_g^+$ of the molecular ion dissociate to the lowest limit $He^+(1s;\ ^2S)+He(1s^2;\ ^1S)$ (see Ref. [5]). As shown by Guberman [4], the dissociative recombination of He_2^+ can take place along several dissociation paths. The most favorable ones, at small electron energies and for ions in low vibrational levels, are members of Rydberg series of the neutral molecule with the dissociative $A\ ^2\Sigma_g^+$ state of He_2^+ as ionization limit. The lowest such state that intersects favorably with the ion ground state is the $^3\Sigma_g^+$ with main configuration $1\sigma_g 1\sigma_u^2 2\sigma_g$. Some of our test calculations are performed with this dissociative curve only, but for the total DR cross section we include also the contribution of the two next dissociative curves (see Fig. 1). The first one corresponds to the $^1\Sigma_g^+$ state with the same orbital configuration as the previous $^3\Sigma_g^+$ state, and lies slightly higher in energy; the second one is the lowest $^3\Pi_u$ dissociative curve with the main configuration $1\sigma_g 1\sigma_u^2 1\pi_u$. This curve lies still higher but is

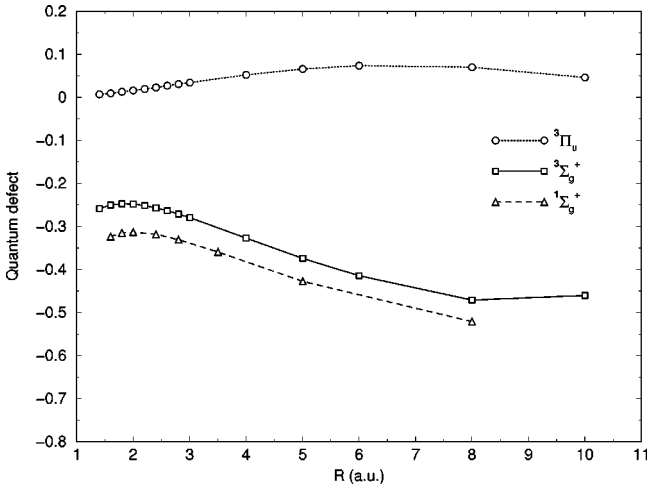

FIG. 2. The quantum-defect functions for the attractive $(X\ ^2\Sigma_u^+)np\sigma_u$ and $(X\ ^2\Sigma_u^+)np\pi_u$ Rydberg states of He_2 with total symmetries $^3\Sigma_g^+$, $^1\Sigma_g^+$, and $^3\Pi_u$, respectively.

strongly coupled to a bound Rydberg manifold of the same symmetry (see Fig. 5 of Ref. [3]), hence to the *p* wave of the incoming electron.

B. Quantum defect functions for bound Rydberg series

In Fig. 1 we also represent, as an example, the first members of the $np\sigma_u$ Rydberg series, with a ground-state ion core and the same symmetry $^3\Sigma_g^+$ as the lowest dissociative state. These states and similar ones for the other symmetries are responsible for the indirect mechanism of DR. We have obtained the relevant quantum defects by performing small configuration-interaction computations on these states. We used the basis described in Ref. [23], to which we added three *s*-type diffuse functions with the exponents 0.061 644, 0.023 709, and 0.009, and three *p*-type diffuse functions with the exponents 0.015, 0.005, and 0.002, to account better for the Rydberg character of the outer electron. The procedure involves the determination, for a set of internuclear distances, of the energy E_n (with *n* the principal quantum number) of the first three members of each Rydberg series, and of its ionization limit $E_{\rm ion}$. The quantum defect functions $\mu(R)$, presented in Fig. 2, are determined by using the molecular Rydberg equation (in a.u.)

$$E_{\rm ion}(R)-E_n(R)=1/2[n-\mu(R)]^{-2},$$

with an average over the three calculated Rydberg states. For the $^3\Sigma_g^+$ symmetry the present result is consistent with the electron scattering calculations of Gillan and co-workers [6] at the equilibrium distance. The same orbital basis was used for the $^1\Sigma_g^+$ Rydberg series, whose quantum defect function behaves very much like that of the triplet series. For the $^3\Pi_u$ states we used an extended He basis with more diffuse orbitals of *d* character. The relatively weak variations of these three quantum defects functions with the internuclear distance indicate that vibrational capture into the bound Rydberg states will be slow, which decides the resonance shape and the global effect of the indirect process, as explained in Sec. IV B below.

C. Electronic couplings

Finally, the MQDT treatment requires electronic couplings responsible for the direct capture into (or autoionization of) the doubly excited dissociative states. For the $^3\Sigma_g^+$ symmetry, we could extrapolate to positive energy the scaled quantity $n^{*3/2}V_n$ (in a.u.), where V_n stands for the electronic interaction between the *n*th Rydberg state of a given series, with the doubly excited state of same symmetry (in a diabatic approach). Indeed, the V_n values obtained by Cohen [3] for $n=3$, 4, and 5 nicely decrease as $n^{*-3/2}$, following the usual behavior for Rydberg series [24].

To obtain the electronic couplings for the two other symmetries involved (only triplet states were studied in Ref. [3], and the coupling values for the $^3\Pi_u$ state are too scarce), and also to check the extrapolated values obtained for the $^3\Sigma_g^+$ state, we performed electron-molecule scattering calculations at three internuclear distances, $R=2.0$, 2.5, and 2.7 a.u. We used the complex Kohn variational method, which we only briefly describe here, and refer the reader to an extensive review [23] for details. We use a trial wave function of the form

$$\Psi_{\Gamma_0}(\mathbf{r}_1,\mathbf{r}_2,\ldots,\mathbf{r}_{N+1}) = \sum_\Gamma \mathcal{A}(\chi_\Gamma(\mathbf{r}_1,\mathbf{r}_2,\ldots,\mathbf{r}_N)F_{\Gamma\Gamma_0}(\mathbf{r}_{N+1})) + \sum_n d_n^{\Gamma_0}\Theta(\mathbf{r}_1,\mathbf{r}_2,\ldots,\mathbf{r}_{N+1}), \quad (3)$$

where the first sum runs over the energetically open target states χ_Γ, $F_{\Gamma\Gamma_0}$ is a one-electron channel orbital antisymmetrized to χ_Γ by the operator $\mathcal{A}$, and Θ_n is an $(N+1)$-electron configuration state function built from square-integrable functions. In the complex Kohn variational method the channel functions are further expanded as

$$F_{\Gamma\Gamma_0}(\mathbf{r}) = \sum_{l,m}[f_l^\Gamma(r)\delta_{ll_0}\delta_{mm_0}\delta_{\Gamma\Gamma_0}+T_{lml_0m_0}^{\Gamma\Gamma_0}g_l^\Gamma(r)] \times\frac{Y_{lm}(\hat{\mathbf{r}})}{r}+\sum_k c_k^{\Gamma\Gamma_0}\Phi_k^\Gamma(\mathbf{r}), \quad (4)$$

where f_l^Γ and g_l^Γ are the regular and outgoing-wave Coulomb functions, and $\Phi_k^\Gamma(r)$ are short-range square integrable functions. To obtain the target state, a set of molecular orbitals were generated from a self-consistent-field calculation using the basis set of Ref. [5]. To represent better the two excited states of the ion, and to obtain a more compact representation for the scattering, a configuration-interaction (CI) calculation on the ion was carried out consisting of all singles and doubles from an active space of two orbitals, $1\sigma_g$ and $1\sigma_u$. Natural orbitals were obtained averaged over the two lowest roots, $(1\sigma_g^2 1\sigma_u)^2\Sigma_u^+$ and $(1\sigma_g 1\sigma_u^2)^2\Sigma_g^+$. The final *target basis* consisted of the four natural orbitals with the highest occupation numbers, two σ_g and two σ_u orbitals. The target

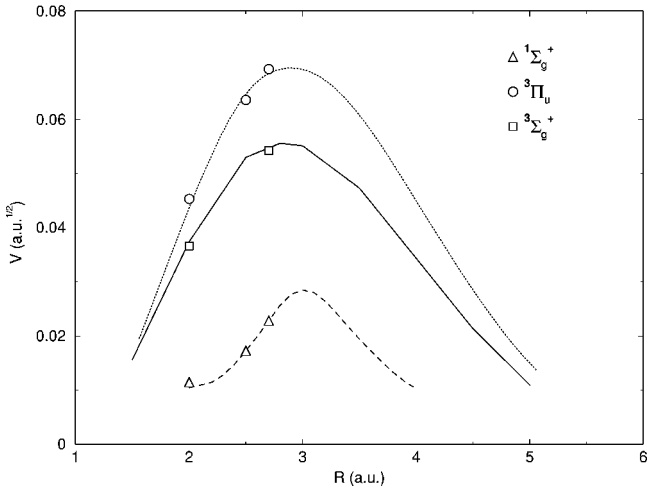

FIG. 3. The electronic coupling functions between the ion ground-state electronic continuum and the $^3\Sigma_g^+$, $^1\Sigma_g^+$, and $^3\Pi_u$ doubly excited states of He_2.

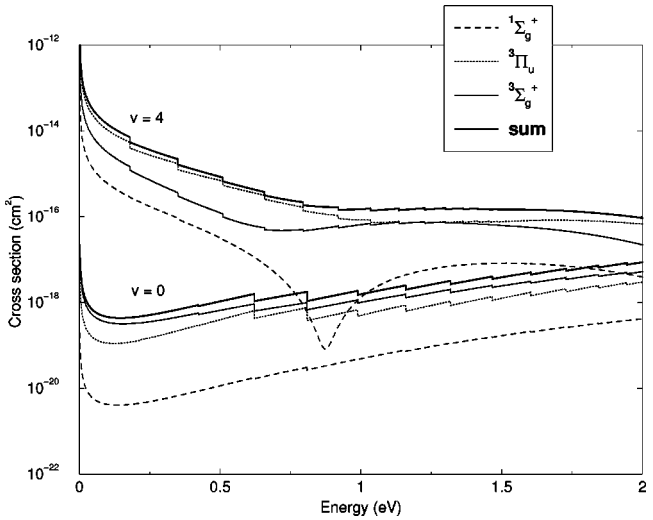

FIG. 4. Contributions of various dissociative states. The DR cross sections for the direct process only, for ($J=0, v=0$) and ($J=0, v=4$) initial rovibrational levels of the molecular ion $^3He^4He^+$ for different dissociative paths (thin lines) and their sum (thick line).

wave functions used in the scattering calculation were obtained by a full CI in the smaller basis of natural orbitals. The target basis was augmented with one diffuse *s* (exponent 0.001), three diffuse *p*'s (exponents 0.05, 0.01, and 0.005) and one *d* (exponent 0.5) Gaussian functions. The variational calculations included continuum basis functions up to $l=|m|=4$. As in previous calculations [23,25] we used Feshbach partitioning to solve the variational equations. Since at the scattering energies considered, only one channel is open, all closed-channel contributions to the first sum in Eq. (3) were combined with the penetration terms to form an effective optical potential.

The calculations were performed in each of the symmetries $^3\Pi_u$, $^3\Sigma_g^+$, and $^1\Sigma_g^+$ for a range of energies around the expected resonance. In each case the eigenphase sum was fitted to a Breit-Wigner form and the resonance parameters, the position $E_{\rm res}(R)$ and width $\Gamma(R)$, were abstracted. Each autoionization width $\Gamma(R)$ is related to the corresponding energy normalized electronic coupling $V(R)$ by the golden-rule formula

$$\Gamma(R)=2\pi V^2(R).$$

The coupling values V thus obtained for the $^3\Sigma_g^+$ states are very close to the extrapolated values $n^{*3/2}V_n$ in the region $R\leqslant 2.74$ a.u., where the scattering calculation can be performed, above the ion curve. As the range of scattering calculations is also limited for the two other states to the intersection point of their potential curves with the ion curve ($R=2.78$ a.u. for the $^1\Sigma_g^+$ state and $R=2.80$ a.u. for the $^3\Pi_u$ state), at larger distance we adopted the same behavior for their coupling functions as for the $^3\Sigma_g^+$ state. In addition, a few checks were possible with extrapolated values from Ref. [3] in the case of the $^3\Pi_u$ state, and with *R*-matrix calculations from Ref. [6] at $R=2.06$ a.u. in the case of the $^1\Sigma_g^+$ state. The results are shown in Fig. 3, with largest coupling values for the $^3\Pi_u$ state, as expected from the smooth adiabatic curves in Fig. 5 of Ref. [3]. Nevertheless, we will see below that this state does not dominate the process at low energy for the lowest vibrational ion level because its intersection point with the ion curve is too high in energy.

IV. RESULTS AND DISCUSSION

We now present the results of our cross-section calculations for different isotopomers of the He_2^+ ion, in various initial rovibrational levels of the electronic ground-state. The intersection point between the lowest dissociative curve and the ion ground state curve is situated well above the minimum of the potential well, between the $v=2$ and 3 outer turning points. For this reason one expects a small cross section for ions in the lowest vibrational levels ($v=0$ and 1) with low rotational excitation, and the DR cross section and rate of He_2^+ should vary strongly with the initial vibrational level of the ion. For each of the three isotopic combinations of ^{3}He and ^{4}He we calculated cross sections for initial vibrational levels ranging from $v=0$ to 4, including the three lowest dissociative states described above. Because the ion vibration level should be easier to control experimentally for the heteronuclear ion, most of our results are shown for the mixed isotope $^3He^4He$. Finally, we tested on this ion the effect of rotational excitation by sampling initial rotational quantum numbers from $J=0$ to 9.

A. Contribution of various dissociative states

In Figs. 4–6 we compare the cross sections obtained for the three lowest dissociation paths, along the $^3\Sigma_g^+$, $^1\Sigma_g^+$, and $^3\Pi_u$ states. The comparison is shown for the heteronuclear $^3He^4He^+$ ion only, and for two different initial vibrational levels $v=0$ and 4 (with $J=0$). The cross sections in Fig. 4 correspond to the direct process only, selected by excluding closed channels from the calculation (each step down seen in the cross sections coincides with the inclusion of a new open channel, i.e., to the threshold for further autoionization competing with DR). For $v=0$ the lowest $^3\Sigma_g^+$ state is dominant, its contribution exceeds the singlet one by

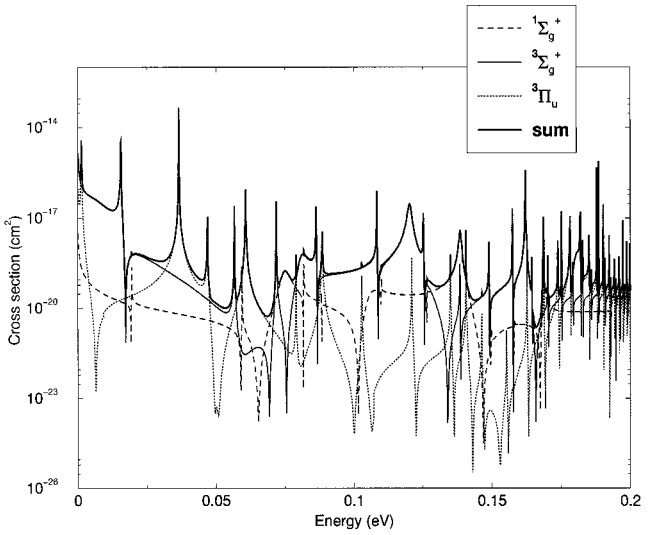

FIG. 5. Same as Fig. 4, for the global (direct plus indirect) DR process and $(J=0, v=0)$ initial ion level.

about two orders of magnitude, due to both a better nuclear overlap (cf. Fig. 1) and a larger electronic coupling (Fig. 3), augmented by a larger multiplicity factor. The contribution of the $^3\Pi_u$ state is intermediate, the effect of its large electronic coupling and multiplicity factor being somewhat compensated for by a smaller nuclear overlap. The situation is very different for the $v=4$ initial vibrational level (upper curves), for which DR is mostly dominated by the contribution of the $^3\Pi_u$ curve, which crosses the ion curve between $v=3$ and 4.

In Figs. 5 and 6 we show (on a smaller energy range) the resonance structure in each individual cross section when the closed channels are included [26]. Except for some resonance energies the relative contributions of the three different states are the same as above. Note the very different aspects of the resonance structures in Figs. 5 and 6, a point which will be discussed in Sec. IV B below.

If we neglect the Σ-Π angular coupling, found by Cohen [3] to be much smaller than the radial ones, the three different dissociation paths do not interfere since they correspond to different symmetries and are not coupled by spin-orbit interaction. The total cross section of DR is then simply the sum of the partial cross sections along each route, and is reported in Fig. 7 for initial levels $v=0$ and 4. At low energy, these three dissociative states certainly account for the whole DR process of He_2^+ ions in low rovibrational levels. Note however, that for higher electron energies or more excited ions $(v>5)$ higher dissociative states should begin to contribute appreciably to the DR process. In particular, the high-energy parts (near 2 eV) of Figs. 4, 8, and 9 should be taken with caution, and only represent the contribution of the lowest dissociative states.

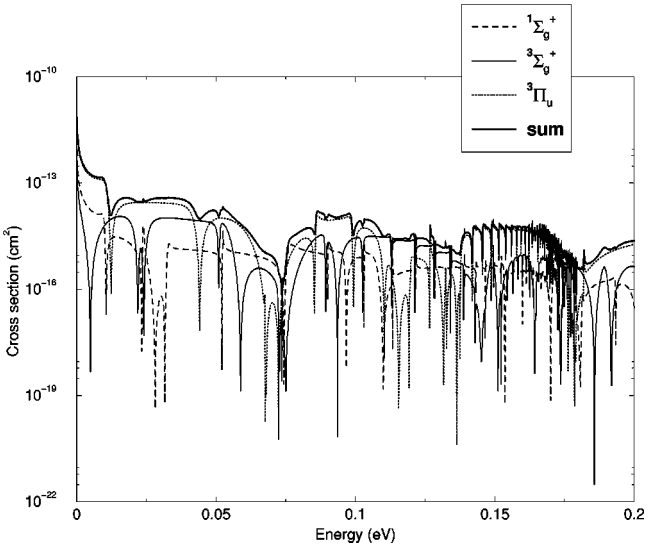

FIG. 6. Same as Fig. 4, for the global (direct plus indirect) DR process and $(J=0, v=4)$ initial ion level.

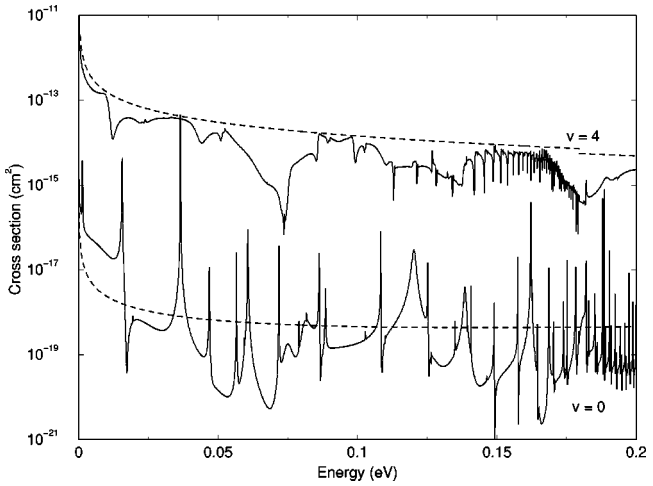

FIG. 7. Effect of the initial vibrational excitation. Total DR cross sections (summed over the three lowest dissociative states) for the $v=0$ and 4 initial vibrational levels (with $J=0$) of the molecular ion $^3He^4He^+$. Dashed lines: direct process only; full lines: direct plus indirect process.

B. Influence of the initial vibrational level

Since $v=3$ is the first vibrational level lying above the intersection point between the lowest dissociative curve and the ion ground state, a significant difference is expected be-

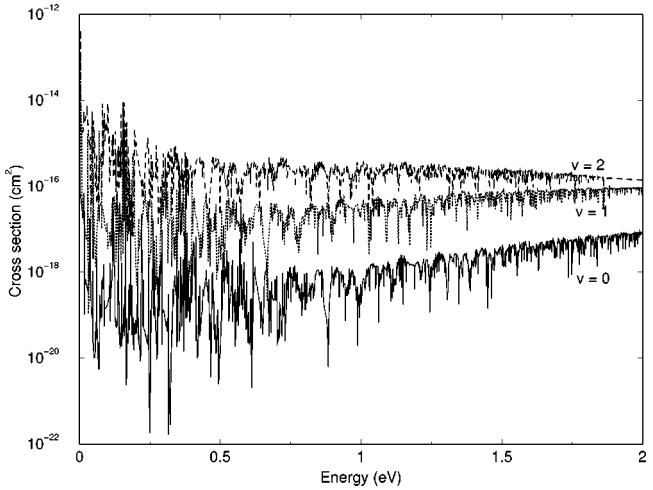

FIG. 8. Same as Fig. 7, on a larger energy range and for the global (direct plus indirect) process. $v=0-2$ initial ion levels (with $J=0$).

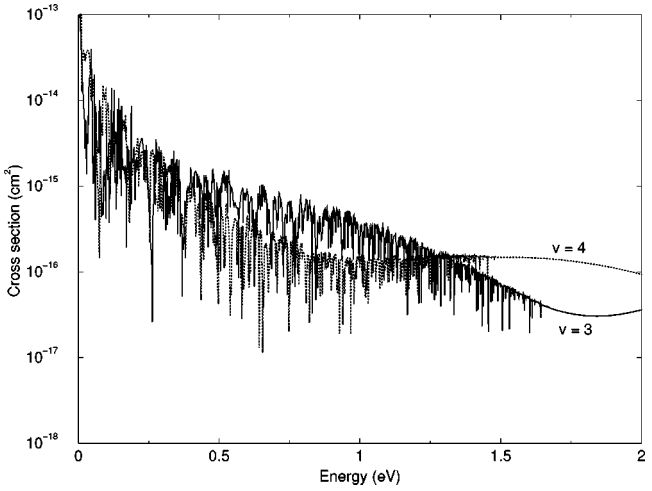

FIG. 9. Same as Fig. 7, on a larger energy range and for the global (direct plus indirect) process. $v=3$ and 4 initial ion levels. Note the different scales for the cross-section values.

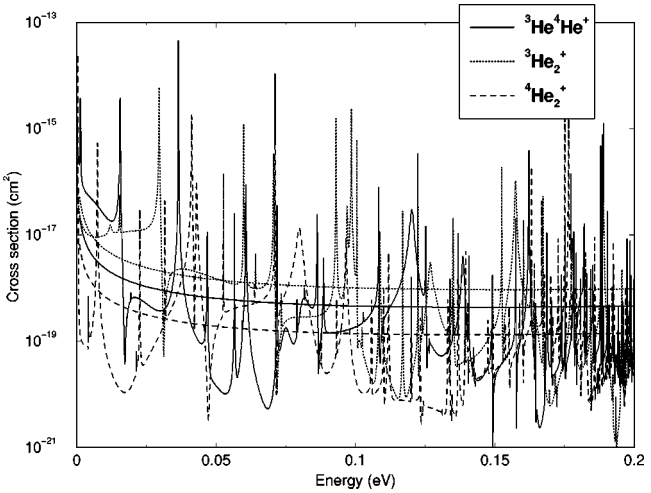

FIG. 11. Same as Fig. 10 for the global (direct plus indirect) process, starting from ($J=0$, $v=0$) initial ion levels.

tween the $v\leqslant 2$ and the $v=3$, and 4 cross sections. Figures 8 and 9 compare them for $^3He^4He^+$, on a large energy range and for the $J=0$ rotational level. At low energy we find about four orders of magnitude increase when going from $v=0$ to 3 initial vibrational levels. However, these cross sections become much closer in magnitude when the electron energy increases, because the $v=0$ ion wave function has a better overlap at higher energy with the dissociative state wave functions. More generally, we find opposite behaviors with increasing energy for the two sets of ion levels, since the $v=0$–2 cross sections (Fig. 8) slowly increase (apart for the resonance structure) between 0.25 and 1 eV, whereas the $v=3$–4 cross sections (Fig. 9) decrease. This comes from opposite variations of the nuclear overlaps with the dissociative states. Above 1.6 eV the $v=0$ and 3 cross sections differ only by a factor of about 2, and at 2 eV the $v=0$–4 cross sections are all within one order of magnitude, between 10^{-17} and 10^{-16} cm^2.

Finally, the aspect of the resonance structure strongly depends on the initial state. This is most clear at low energy, comparing the resonance shapes for $v=0$ (Fig. 5) and $v=4$ (Fig. 6), summarized for total cross sections in Fig. 7. For $v=0$ most of the resonances appear as a peak followed by a dip (exaggerated by the logarithmic scale), while, for $v=4$, the resonances are mainly in form of dips. This reveals different interference pattern between the direct and indirect processes. For the $v=0$ initial level, both the direct and indirect processes are weak, and they interfere in an intermediate regime, leading to an asymmetric resonance shape with a Fano parameter larger than 1, in favor of constructive interference. Conversely, the fast direct DR for the $v=4$ initial level (see Fig. 4) is hindered by slow vibrational capture into a bound Rydberg state, leading to window resonances with q Fano parameter close to zero (destructive interference).

It may be noted in Figs. 8 and 9 that for the highest v, above a given energy of the incident electron (about 1.5 eV for $v=4$, 1.7 eV for $v=3$, and 1.9 eV for $v=2$), the resonance structure vanishes in the cross section. Indeed, the total energy then exceeds the ion dissociation limit and all the ionization channels become open, which stops the indirect

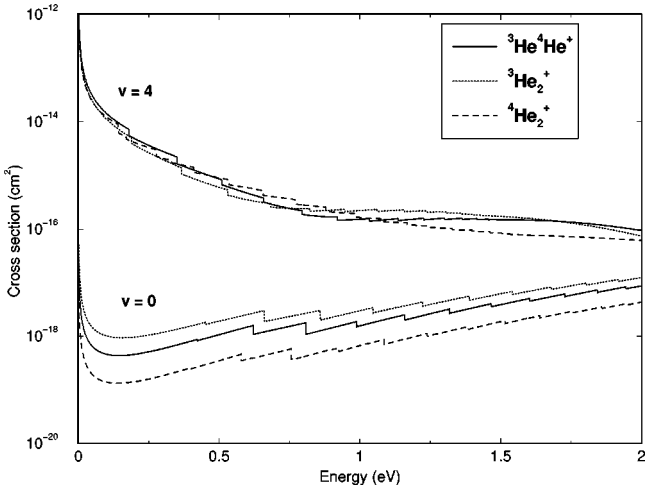

FIG. 10. Isotopic effect. Comparison between the direct DR cross sections (sum over the three lowest dissociative states) for the molecular ions $^3He^4He^+$, $^4He_2{}^+$, and $^3He_2{}^+$, respectively.

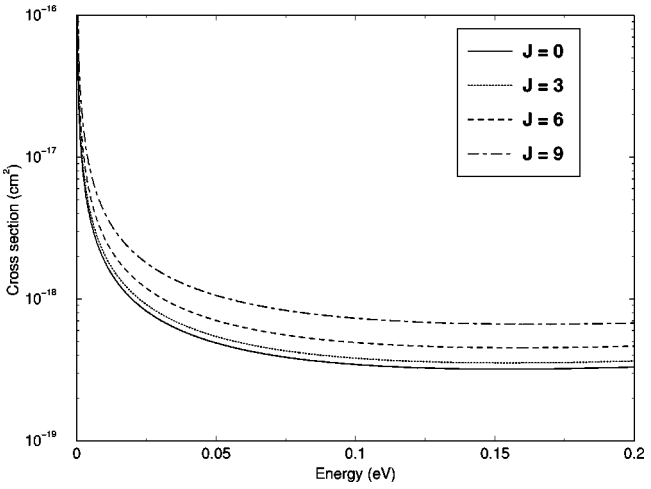

FIG. 12. Effect of rotational excitation. DR cross sections for the direct process only, for $^3He^4He^+$ in different initial rotational levels J with $v=0$. For these test calculations only the $^3\Sigma_g^+$ dissociative state has been included.

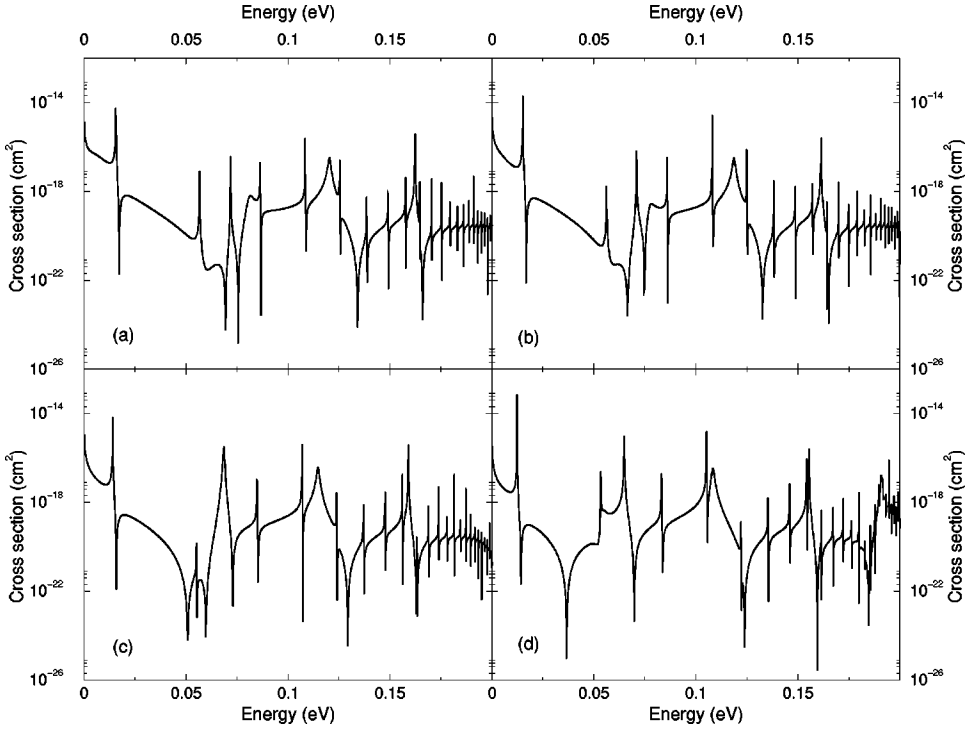

FIG. 13. Same as Fig. 12, for the global (direct plus indirect) DR process, starting from different initial rovibrational levels: (a) $J=0, v=0$; (b) $J=3, v=0$; (c) $J=6, v=0$; and (d) $J=9, v=0$.

DR mechanism described in Sec. II. The same would happen to the $v=0$ and 1 cross sections at slightly higher energy, about 2.1 eV for $v=1$ and 2.3 eV for $v=0$ (the exact values depending on the isotope). Just below each of these thresholds the Rydberg resonances become very narrow (high-n values) and compressed, and will be washed out in any average, such that no sudden change should be observed in experimental cross sections or rates.

C. Isotopic effect

In Figs. 10 and 11 we compare total cross sections for the three isotopomers $^3He_2^+$, $^4He_2^+$, and $^3He^4He^+$, for initial rovibrational levels ($J=0$, $v=0$) and ($J=0$, $v=4$) of the ion ground state. In spite of quantitative differences due to different nuclear overlaps we observe similar behaviors for the various *direct* cross sections (Fig. 10), all within less than one order of magnitude. The resonance energies and shapes in the total cross sections (Fig. 11) change from one isotope to another due to changes in the vibrational spacings, and at very small energies the three cross sections are very different due to resonances lying just at threshold with different interference pattern, but the general picture is the same. This implies that the isotopic effect, in addition to the presence of the permanent dipole in the $^3He^4He$ molecule (which can prove decisive for the experiments, as explained earlier), has little influence on the average DR cross section, which is mostly dominated by electronic interactions.

D. Influence of the initial rotational level

As a last test, we performed cross-section calculations for a sample of the initial rotational levels of the ground state ion $^3He^4He^+$ with $v=0$, including the contribution of the lowest dissociative state only. The cross sections for the direct process (Fig. 12) as well as the total one (direct plus indirect, Fig. 13) show very little change between $J=0$ and 3, but significant differences are found for the higher values of J. The direct cross section increases roughly by a factor 2 when going from $J=0$ to 9, and the resonance structure in the total cross section is modified due to energy changes for the resonant bound states.

When averaged over a Boltzmann distribution of rotational levels the resulting cross section is very close to the $J=0$ one for $T=300$ K (Fig. 14), where the distribution peaks at $J=3$, while at 2000 K (Fig. 15), with a peak at J

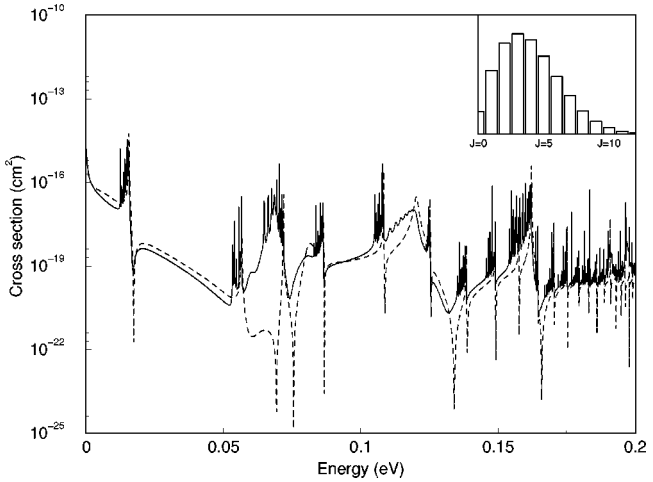

FIG. 14. Averaged DR cross section (contribution of the $^3\Sigma_g^+$ dissociative state only) for $^3He^4He^+$ molecular ions in a Boltzmann distribution of rotational levels at 300 K, with $v=0$. The inset shows the corresponding Boltzmann distribution of initial rotational levels. The dashed line reports the $J=0$ cross section [Fig. 13(a)] for comparison.

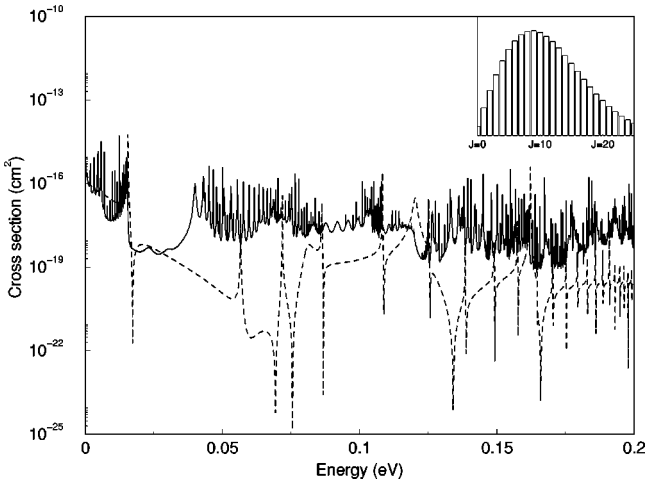

FIG. 15. Same as Fig. 14 for $T=2000$ K.

$=9$, it is larger for most of the energy range studied. This is an indication that rotational excitation should be taken into account for a precise comparison with experiments in which molecular ions are injected with high internal energy.

E. Final atomic states

In flow-tube experiments radiation from excited final states resulting from DR can help in analyzing the results and determining the DR cross section. In addition, recent DR experiments in ion-storage rings have been able to measure branching ratios into the final atomic fragments [14,15]. Although the calculations presented here do not explicitly determine the final states, certain predictions can be made from asymptotic correlations of the three dissociative states involved. All correlate with one helium atom in the $He(1s^2;\ ^1S)$ ground state and the other one in a metastable state: $He(1s2s;\ ^3S)$ for the $^3\Sigma_g^+$ state, $He(1s2s;\ ^1S)$ for the $^1\Sigma_g^+$ state, and finally $He(1s2p;\ ^3P)$ for the $^3\Pi_u$ dissociative state. Therefore, in the absence of curve crossings in the asymptotic region, one would expect only a ground state and metastable He final states. As indicated by Guberman and Goddard [27], there is a curve crossing between the $^1\Sigma_g^+$ states arising asymptotically from ground-state He and either $He(1s2s;\ ^1S)$ and $He(1s2p;\ ^1P)$. This crossing could result in some transfer from the metastable $He(1s2s;\ ^1S)$ state to the $He(1s2p;\ ^1P)$ state which can be optically observed. However, especially at low energy and for the first ion vibrational levels $v=0$–2, the dissociative $^1\Sigma_g^+$ channel is of minor importance; hence also the production of the $He(1s2p;\ ^1P)$ final state.

V. CONCLUSION

In summary, the following results have been obtained. First, alternative routes for low-energy dissociative recombination of He_2^+ molecular ions are possible, and the dominant one depends strongly on the energy and the initial rovibrational level. The lowest $^3\Sigma_g^+$ state is the most effective dissociation path at very low energy and for the $v=0$–2 vibrational levels, whereas for $v=3$–4 the DR mainly occurs along the first $^3\Pi_u$ repulsive curve, and also a Rydberg state with the $A^2\Sigma_g^+$ state as ion core. Second, the initial rovibrational level of the molecular ion strongly influences the dissociative recombination cross section at low energy. The difference between the $v=0$ and 3 average cross sections is about four orders of magnitude below 1 eV, for each of the three isotopomers we have studied. This difference decreases at higher collision energy, due to a better nuclear overlap between the $v\leqslant 2$ ion vibrational wave functions and the dissociative ones. Around 2 eV the $v=0$–4 cross sections are all within one order of magnitude, an important feature for experiments attempting to test the initial ion level by comparing heteronuclear and homonuclear ion results. Although the mixed isotopomer $^3He^4He^+$ should relax much more quickly to the ground level, the measured cross sections could differ only slightly except at low energy. Finally, the resonance structure induced by the indirect DR process is very sensitive both to the initial rovibrational level and to the dissociation channel, with the general tendency to slow down the fast processes by destructive interferences and to slightly speed up the slower ones.

So far no absolute values for the DR cross section of He_2^+ have been reported. Relative measurements for $^4He_2^+$ and the mixed variety $^3He^4He^+$ are being performed in Aarhus on the ASTRID storage ring [9], on a much larger energy range (up to 20 eV) than for the present calculations. The only published experimental results for He_2^+ DR are rates determined in plasma afterglows. Due to the complexity of the phenomena in such plasmas, the reports were somewhat controversial but the rate of DR at 300 K was found to be less than 5×10^{-10} $cm^3\,s^{-1}$ [7] for $^4He_2^+$ ions. The present calculations lead to cross-section values around 10^{-18} cm^2 near 0.026 eV for $(J=0,\ v=0)$ initial level (see Figs. 10 and 11), and the corresponding rate coeficient can be fitted to the relation

$$\alpha=1.04\times10^{-8}T^{-0.9}\ \ cm^3\,s^{-1}.$$

in the temperature range 250–350 K. Its value at 300 K is 6.1×10^{-11} $cm^3\,s^{-1}$, consistent with the low measured rates. However, this does not rule out the possible contribution of nonadiabatic couplings to low-lying dissociative states, below the ion curve. This type of mechanism, not included in the present calculation, has been found to be important in the case of HeH^+ [28,29]. Here we do not expect a significant increase of the cross section, but it could direct part of the flux to lower dissociation limits, including totally ground-state products. Recent experiments by Hardy [30] have seen evidence of the production of He atoms on the ground potential-energy curve of the neutral, and we are currently investigating this possibility.

ACKNOWLEDGMENTS

We warmly thank K. Hardy, J. Peterson, I.F. Schneider, and X. Urbain for fruitful discussions. A.E.O. and L.C. acknowledge support from the National Science Foundation under Grant No. PHY-97-22136. A.E.O. received partial support from the Lawrence Livermore Research Collaborations Program for Historically Black Colleges and Universities and Minority Institutions. Part of this work was performed under the auspices of the U.S. Department of Energy at the Lawrence Livermore National Laboratory, under Contract No. W-7450-Eng-48.

[1] D. R. Bates, Phys. Rev. **77**, 718 (1950).
[2] E. E. Ferguson, F. C. Fehsenfeld, and A. Schmeltekopf, Phys. Rev. A **138**, 381 (1965).
[3] J. S. Cohen, Phys. Rev. A **13**, 86 (1976).
[4] S. L. Guberman, in *Physics of Ion-Ion and Electron-Ion Collisions*, Vol. 83 of *NATO Advanced Study Institute Series B: Physics*, edited by F. Brouillard and J. W. McGowan (Plenum, New York, 1983), p. 167.
[5] K. K. Sunil, J. Lin, H. Siddiqui, P. E. Siska, and K. D. Jordan, J. Chem. Phys. **78**, 6190 (1983).
[6] C. J. Gillan, B. M. McLaughlin, and P. G. Burke, in *Dissociative Recombination: Theory, Experiments and Applications II*, Vol. 313 of *NATO Advanced Study Institute Series B: Physics*, edited by B. Rowe, J. B. A. Mitchell, and A. Canosa (Plenum, New York, 1993), p. 155; B. M. McLaughlin, C. J. Gillan, P. G. Burke, and J. S. Dahler, Phys. Rev. A **47**, 1967 (1993).
[7] R. Deloche, P. Monchicourt, M. Cheret, and F. Lambert, Phys. Rev. A **13**, 1140 (1976).
[8] V. A. Ivanov and Yu. E. Skoblo, Opt. Spektrosk. **65**, 750 (1998) [Opt. Spectrosc. **65**, 445 (1988)].
[9] X. Urbain and L. H. Andersen (unpublished).
[10] P. Forck *et al.*, Phys. Rev. Lett. **70**, 426 (1993).
[11] T. Tanabe *et al.*, Phys. Rev. Lett. **75**, 1066 (1995).
[12] C. Strömholm *et al.*, Phys. Rev. A **52**, R4320 (1995).
[13] L. H. Andersen *et al.*, Phys. Rev. A **55**, 2799 (1997).
[14] Z. Amitay *et al.*, Science **281**, 75 (1998).
[15] M. Larsson, Annu. Rev. Phys. Chem. **48**, 151 (1997).
[16] A. Suzor-Weiner and I. F. Schneider, in *Dissociative Recombination: Theory, Experiments and Applications III*, edited by D. Zajfman, J. B. A. Mitchell, D. Schwalm, and B. R. Rowe (World Scientific, Singapore, 1996), p. 1; L. Carata, I. F. Schneider, and A. Suzor-Weiner, Philos. Trans. R. Soc. London, Ser. A **355**, 1677 (1997).
[17] A. Giusti-Suzor, J. Phys. B **13**, 3867 (1980).
[18] S. L. Guberman and A. Giusti-Suzor, J. Chem. Phys. **95**, 2602 (1991).
[19] H. Takagi, J. Phys. B **26**, 4815 (1993).
[20] I. F. Schneider, C. Strömholm, L. Carata, X. Urbain, M. Larsson, and A. Suzor-Weiner, J. Phys. B **30**, 2687 (1997).
[21] B. Vâlcu, I. F. Schneider, M. Raoult, C. Strömholm, M. Larsson, and A. Suzor-Weiner, Eur. Phys. J. D **1**, 71 (1998).
[22] J. S. Cohen, Phys. Rev. A **13**, 99 (1976).
[23] A. Orel, T. N. Rescigno, and B. H. Lengsfield III, Phys. Rev. A **44**, 4328 (1991).
[24] J. N. Bardsley, Chem. Phys. Lett. **1**, 229 (1967); J. Phys. B **2**, 365 (1968).
[25] T. N. Rescigno, C. W. McCurdy, A. E. Orel, and B. H. Lengsfield III, in *Computational Methods for Electron-Molecule Collisions*, edited by W. M. Huo and F. A. Gianturco (Plenum, New York, 1995).
[26] The total number of ionization channels (open plus closed) included in a complete calculation is 18 for $^3He_2^+$, 19 for $^3He^4He^+$, and 22 for $^4He_2^+$, corresponding to the respective number of vibrational levels in the ground-state potential well (with $J=0$).
[27] S. L. Guberman and W. A. Goddard III, Chem. Phys. Lett. **14**, 460 (1972).
[28] S. L. Guberman, Phys. Rev. A **49**, R4277 (1994).
[29] B. K. Sarpal, J. Tennyson, and T. A. Morgan, J. Phys. B **27**, 5943 (1994).
[30] K. Hardy (private communication).